

Article

Annealing Behavior of 6061 Al Alloy Subjected to Differential Speed Rolling Deformation

Young Gun Ko ¹ and Kotiba Hamad ^{2,*}

¹ School of Materials Science and Engineering, Yeungnam University, Gyeongsan 38541, Korea; younggun@ynu.ac.kr

² School of Advanced Materials Science and Engineering, Sungkyunkwan University, Suwon 16419, Korea

* Correspondence: hamad82@skku.edu; Tel.: +82-31-290-7401

Received: 27 October 2017; Accepted: 6 November 2017; Published: 10 November 2017

Abstract: This study investigated the effects of heat treatment (annealing) on the microstructure of ultrafine grained 6061 Al alloy samples fabricated by a differential speed rolling (DSR) process. The samples were fabricated using two passes DSR with 75% thickness reduction and a speed ratio of 1:4. The DSR-deformed 6061 Al alloy sample exhibited a lamellar boundary structure composed mostly of subgrains surrounded by low-angle grain boundaries. After annealing, the DSR-deformed 6061 Al alloy samples exhibited coarse grained structure and transformed from lamellar to equiaxed, where both the grain size and grain shape aspect ratio increased with increasing annealing temperature. The fraction of grain boundaries with high misorientation angles increased progressively during annealing, to ~77% at annealing temperature of 350 °C.

Keywords: differential speed rolling; 6061 Al alloy; annealing; microstructure

1. Introduction

The interest in ultrafine grained (UFG) materials with exceptional properties has increased rapidly because of their scientific and technological importance. In recent studies, metals with an UFG structure (mean grain size < 1 μm) showed extraordinary performance, such as improved strength and low-temperature super-plasticity [1,2]. One method to achieve the UFG structure is severe plastic deformation (SPD). Several methods have been applied successfully to fabricate UFG materials using SPD. Those are equal-channel angular pressing (ECAP), accumulative roll bonding (ARB), high pressure torsion (HPT) and differential speed rolling (DSR) [3–9]. Among them, DSR is the method that shows a high capability to produce UFG sheets continuously. This is usually carried out by imposing uniform shear strain in the thickness direction of the sheets through two identical rolls with different rotation speeds [7–9].

Aluminum alloys are used for applications such as food packaging, sports utilities, automotive and aircraft because of their high specific strength (strength/density ratio) and corrosion resistance. Alloys with the base composition of ternary aluminum-magnesium-silicon, which are called 6xxx series, possess good strength, heat-treatability, excellent formability and acceptable corrosion resistance [10]. In this series, 6061 Al alloy is the most commonly used alloy in many applications and can be fabricated easily by extrusion, forging or rolling. To enhance the property of the 6061 Al alloy for specific applications, grain refinement is used. Kim et al. [11] reported that the mechanical properties of UFG 6061 alloy subjected to DSR deformation was higher than those fabricated by ECAP and HPT.

The excellent strength achieved after deformation by DSR is usually conjugated with the poor ductility which has limited the material applicability in the industrial fields. For improving the strength and ductility of the UFG materials, an appropriate thermal treatment following plastic deformation is required. Several studies examining the effects of annealing have been carried out. Kim et al. [12] reported that the thermal treatment of an ECAP deformed 6061 Al alloy was effective in improving

the strength whilst retaining moderate tensile ductility. Rezaei et al. [13] reported the improved performance (strength and ductility) of ARB-deformed sheets after a thermal treatment. On the other hand, there has been no conclusive research on the microstructural evolution of UFG 6061 Al alloy deformed by DSR during annealing. Therefore, the aim of this work is to investigate microstructural evolution of DSR-deformed 6061 Al alloy during annealing.

2. Experiments

The chemical composition of the 6061 Al alloy sheets used in the present work was (in wt %): 0.9 Mg, 0.71 Si, 0.5 Fe, 0.24 Cu, 0.19 Cr, 0.12 Mn, 0.05 Zn, 0.05 Ti, with Al comprising the balance. The as-received sheets were cut into small plates, 0.4 cm (thickness), 4 cm (width) and 10 cm (length). The plates were then homogenized for 3 h at 550 °C and air cooled to obtain a fully annealed structure (Figure 1). The homogenized plates were then subjected to the room-temperature DSR deformation using two identical rolls (220 mm in diameter). To impose the shear deformation by DSR, a speed ratio of 1:4 was used, where the lower roll speed was fixed to ~3 m/min. The plates were subjected to two passes with 50% thickness reduction per pass, so that the total thickness reduction was 75% after the DSR deformation (two passes). During the DSR deformation, the plates were rotated by 180° around their rolling direction between the adjacent passes. This route was found to be beneficial for controlling the material with a fine grain structure [14,15]. The heat treatment was carried out on the DSR-deformed plates for 1 h at various temperatures of 150–400 °C with an interval of 25 °C.

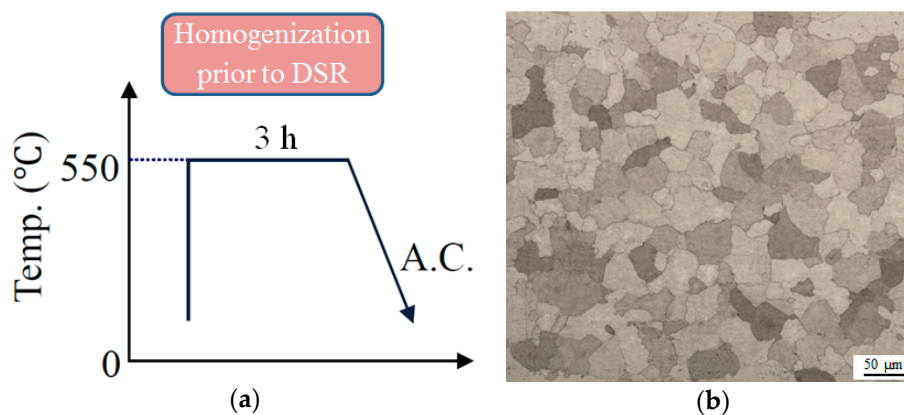


Figure 1. (a) Homogenization conditions of the as-received 6061 Al alloy sheets and (b) the obtained microstructure (DSR: Differential Speed Rolling; A.C.: Air Cooled).

The structural features of the deformed and annealed plates were observed using electron backscatter diffraction (EBSD, Hitachi S-4300 FESEM; Hitachi, Tokyo, Japan). For EBSD observations, sample cut from the normal direction-rolling direction (ND-RD) plane, were electro-polished using a solution of 20% perchloric acid in methanol at 25 V for 10 s. The EBSD observations were conducted at a step size of 0.02 μm. The EBSD data was analyzed using a TSL OIM 6.1.3 (Hitachi, Tokyo, Japan) and the evaluation of misorientation distribution was made based on the assumption that the misorientation angles from 2° to 15° indicated the low angle-grain boundaries (LAGBs) whereas the misorientation angles higher than 15° implied the high-angle grain boundaries (HAGBs). Transmission electron microscopy observations (TEM, Philips TECNAI G2F20; Drachten, The Netherlands) of the annealed plates were performed at an acceleration voltage of 200 kV. For this measurement, foils cut from the annealed plates were thinned by a focused ion beam. To measure the Vickers microhardness, the annealed 6061 Al alloy plates with mirror-like surfaces were tested under a load and dwell time of 200 g and 10 s, respectively. In order to avoid the occurrence of natural aging, the microstructure observations and hardness measurements were carried out right after deformation and annealing experiments.

3. Results and Discussion

3.1. Microstructural Features of the Differential Speed Rolling-Deformed 6061 Al Alloy

Figure 2 shows the EBSD maps obtained from the near-surface region of the 6061 Al alloy plate deformed by the DSR under the investigated conditions (two passes, 75% and 1:4). The EBSD maps (inverse pole figure (IPF) and grain boundaries (GBs)) in Figures 2a and 1b show a lamellar boundary structure composed mostly of subgrains with high fraction of low-angle grain boundaries (LAGBs), as shown by the dashed rectangle A in Figure 2a. In addition, a lower fraction of ultrafine grains surrounded by boundaries with an angle of misorientation ($>15^\circ$) are also observed near the lamellar boundaries (dashed rectangle B in Figure 2a). This was also confirmed by the grain boundaries map presented in Figure 2b.

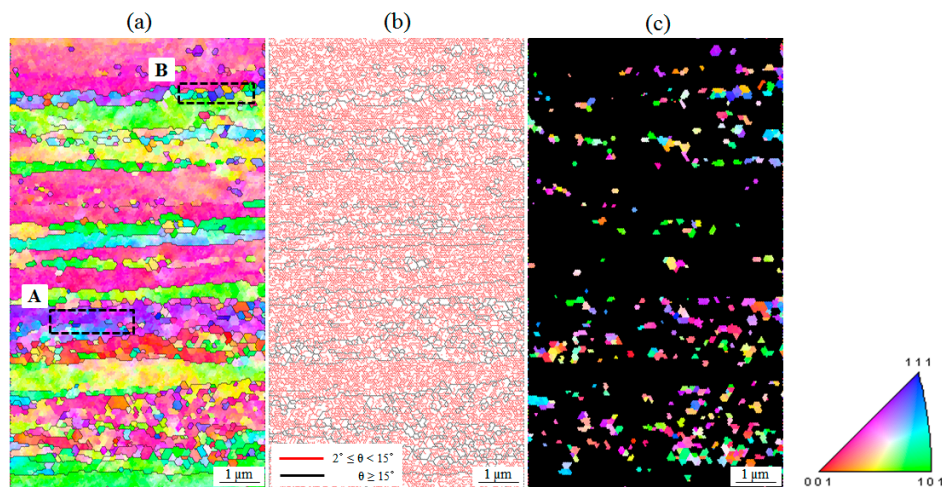


Figure 2. (a) IPF (Inverse Pole Figure), (b) grain boundaries and (c) partitioned IPF maps of the DSR-deformed 6061 Al alloy.

The nucleation of such ultrafine grains around the elongated grains leads to a necklace-like structure, which was also reported in bcc materials after deformation by DSR at different thickness reductions [16,17]. The evolution of the necklace-like structure is typical of a continuous dynamic recrystallization (CDRX) process at an intermediate stage of deformation by SPD [18]. This can be attributed to the rapid evolution of strain gradients near grain boundaries, leading to the formation of large misorientations in the vicinities of the boundaries. Therefore, it is deduced that different grain refinement mechanisms can occur, depending on the materials and processing conditions.

The fraction of ultrafine grains (~23%) in the deformed microstructure was determined by partitioning the ultrafine grains using the criteria of the grain orientation spread (GOS) [19], as shown in Figure 2c. In addition, the individual layers formed between the lamellar boundaries were characterized by low-angle grain boundaries (LAGBs) and intra-layer orientation gradients resulting in the (sub) grain structure. After the DSR deformation, the presence of LAGBs inside the elongated grains is normally observed after SPD deformation. To explain the development of the (sub) grained structure inside the individual layers, the misorientation profiles were recorded along the rectangle A in Figure 2a. The misorientation profiles (point-to-origin and point-to-point) measured along the dashed line (L) are presented in Figure 3. The results showed large variation across the individual layer, where average values of 4.06° and 6.77° were recorded for point-to-origin and point-to-point misorientation, respectively. The increase in the intra-layer misorientation is associated with the formation of a (sub) grain structure. On the other hand, low misorientation regions in this profile are associated with the formation of dislocation-cell structure. Based on the EBSD measurements of the DSR-deformed sample, it is worth pointing out that the traditional definition of the grain size

is not enough here, where sub structures with clear orientation gradients are formed after the DSR deformation. Due to these gradients, two (non-neighboring) points belonging to the same grain can be highly misoriented. Consequently, the calculation of grain size may characterize both grains and subgrains. The distribution of the (sub) grain size of the 6061 Al alloy deformed by the DSR process (Figure 4a) shows that a significant fraction (~19%) of grains have diameters less than 0.1 μm , whereas the average diameters (d_{ave}) lies within 0.4–0.5 μm . In addition, ~40% of the grain boundaries have misorientation angles higher than 15° (high-angle grain boundaries (HAGBs)), as shown by Figure 4b.

The precipitation behavior of 6061 Al alloy subjected to DSR deformation was investigated by Kim et al. [11]. They found that the features of precipitates after the DSR deformation, including number, size, shape and distribution, are mainly related to the initial microstructure (before deformation). Their results revealed that the sample with a fully-annealed structure possessed a small number of precipitates after the DSR deformation. In the presented work, accordingly, the sample was subjected to a heat treatment at 550 °C for 3 h followed by air cooling to obtain a fully-annealed structure (Figure 1). In addition, the rolling temperature (RT) employed here is a less than ideal aging temperature of 6061 Al alloy (~170 °C).

Based on this discussion, it can be noted that the effect of the DSR deformation and pre/post heat treatment on the precipitation behavior of Al alloys should be investigated in more detail using high resolution TEM.

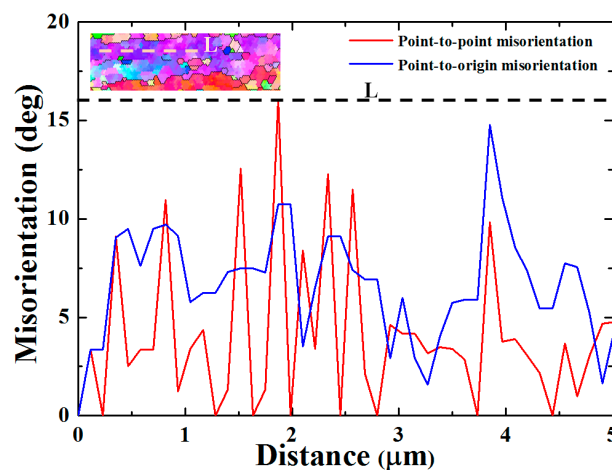


Figure 3. Misorientation profile along the dashed line taken from the rectangle A in the DSR-deformed 6061 Al alloy (Figure 2a).

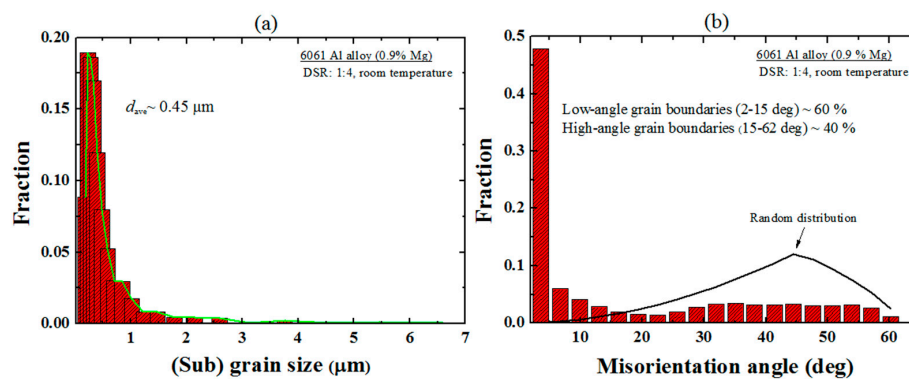


Figure 4. (a) Grain size distribution and (b) grain boundaries misorientations of the DSR-deformed 6061 Al alloy. The green line in Figure 4a shows additionally the grain size distribution.

3.2. As-Annealed Samples

3.2.1. Microhardness

Figure 5a shows microhardness of the DSR-deformed 6061 Al alloy samples as a function of the annealing temperature. The curve obtained in Figure 5a exhibited the following three different regions (i) the microhardness decreases slightly until ~ 225 °C. This range corresponds to the recovery in the materials. (ii) The microhardness decreases sharply, i.e., at a steeper slope on the curve, from 225 to 350 °C and (iii) the curve levels off at temperatures higher than 350 °C. The sharp decrease of the microhardness in the second region of the curve suggests the occurrence of material softening induced by recrystallization [20]. To show the effect of the annealing temperature on the softening behavior of the DSR-deformed 6061 Al alloy, the softened fraction (X) was calculated as follows [21,22]:

$$X = \frac{H_d - H_t}{H_d - H_0} \quad (1)$$

where H_d , H_t and H_0 are the microhardness after DSR deformation, the instantaneous microhardness at any temperature, and the microhardness of the initial sample prior to DSR, respectively. Figure 5b shows the softened fraction at the various annealing temperatures used in this work. After annealing at 225 °C for 1 h, the estimated softened fraction of the annealed sample showed a $\sim 2.99\%$ reduction compared to the DSR-deformed sample. The softened fraction of the sample increased significantly after annealing at temperatures between 225 and 350 °C, where the samples annealed at 275, 325 and 350 °C showed $\sim 45\%$, $\sim 79.8\%$ and $\sim 99.8\%$ softened fraction compared to the as-deformed sample.

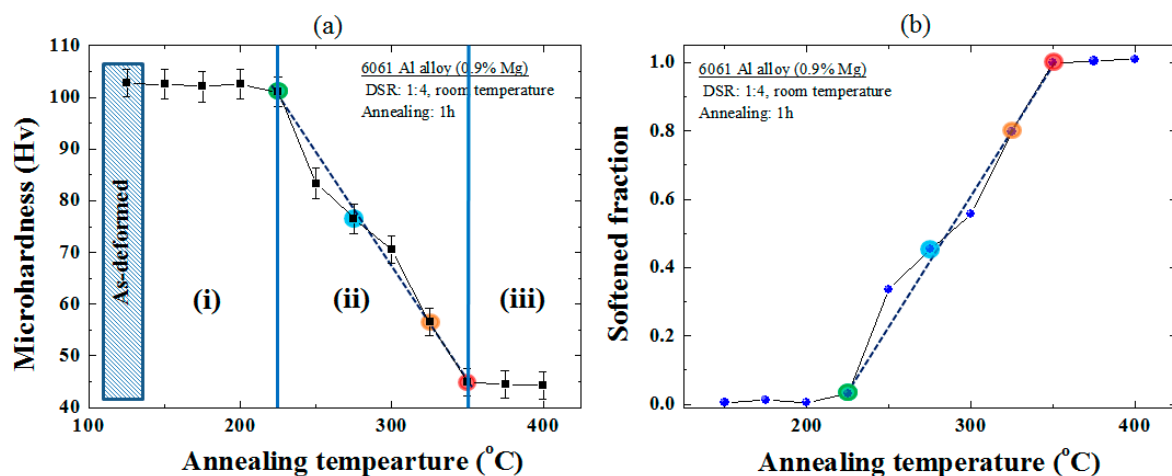


Figure 5. Effect of the annealing temperature on (a) microhardness and (b) softened fraction of the DSR-deformed 6061 Al alloy. The different color remarks along the dashed line in this figure indicate the annealed samples used to investigate the microstructural evolution during annealing.

3.2.2. Microstructure

The microstructural evolution of the samples annealed at 225 °C, 275 °C, 325 °C and 350 °C, which belong to the second region (ii) as indicated by the colored symbols in Figure 5a, were investigated to understand the softening behavior of the DSR-deformed 6061 Al alloy plates during the heat treatment. The EBSD maps (grain boundaries maps) in Figure 6 showed that the lamellar structure was gradually broken-down to form the equiaxed grains. On the other hand, at 275 °C, some areas showed the lamellar structure obtained by the initial DSR deformation, as indicated by the dashed rectangles in Figure 6b. This was shown further by partitioning of the recrystallized grains of the samples treated at 225, 275, 325 and 350 °C using the criteria of GOS [19] (Figure 6e–h). The most obvious and expected observation from Figure 6e–h is that the fraction of the recrystallized grains increased with increasing

the temperature, where recrystallizations corresponding to ~18%, ~31%, 52% and ~84% were measured after the heat treatment at 225, 275, 325 and 350 °C, respectively. In addition, the larger fraction of recrystallized microstructures of the sample annealed at 350 °C (Figure 6h) resulted in the low microhardness values, as shown in Figure 5a.

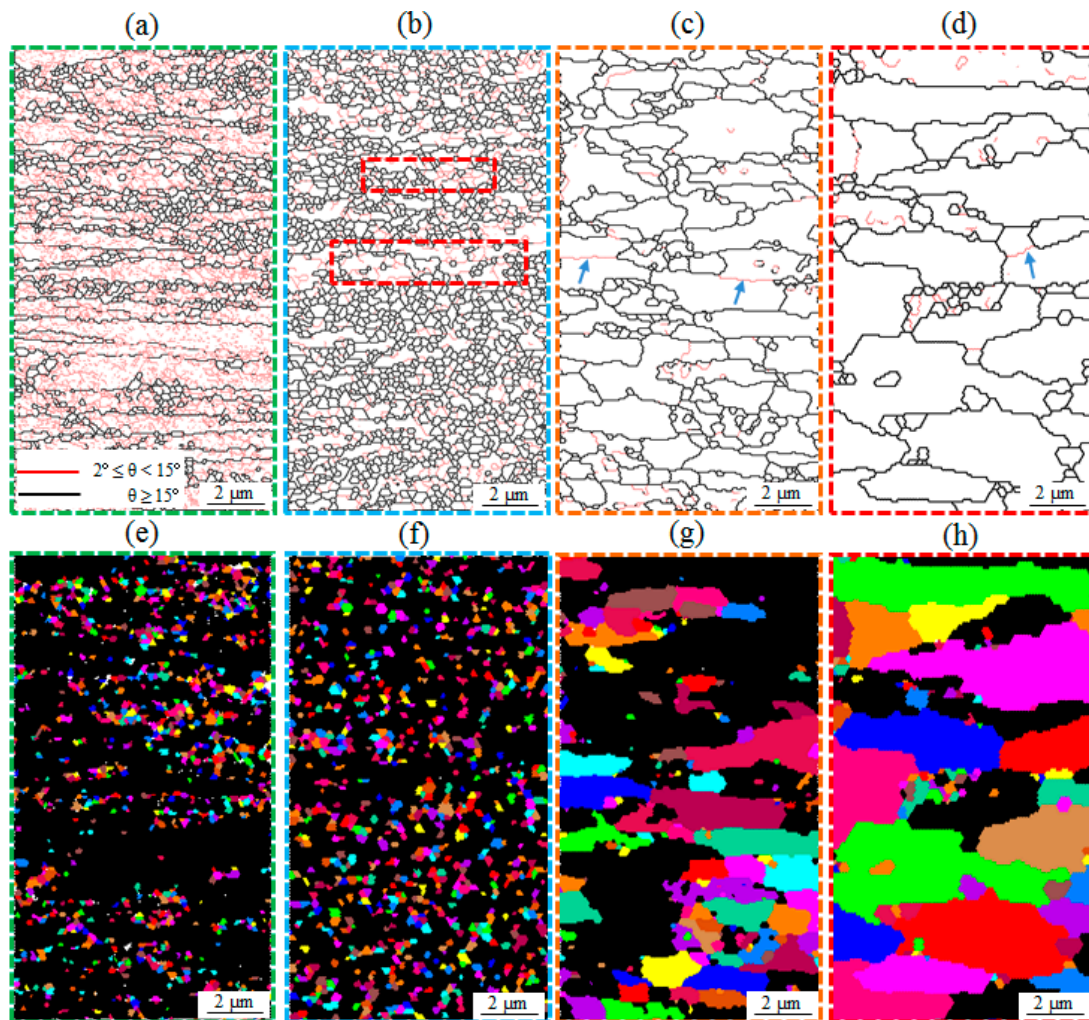


Figure 6. Grain boundaries maps and recrystallized microstructures of the DSR-deformed 6061 Al alloy annealed for 1 h at (a,e) 225 °C (b,f) 275 °C (c,g) 325 °C (d,h) 350 °C.

Figure 7 presents the microstructural parameters of the annealed plates, including the grain size, grain shape aspect ratio and grain boundary misorientations. The grain size distributions of the annealed plates shown in Figure 7b clearly show that after annealing at 225 °C and 275 °C for 1 h, the grain size increased from ~0.9 μm, which are still submicron grains, to ~2.2 μm (Figure 7b,d). After annealing at 325 °C and 350 °C, a significant change in grain morphology was observed, where equiaxed grains with shape aspect ratios of 0.6 and 0.62 were obtained after annealing at 325 °C and 350 °C, respectively (Figure 7a,d). The distributions of the grain boundary misorientations in Figure 7c revealed that the fraction of HAGBs evolved during the heat treatment of the deformed plates increased with increasing the temperature, where ~44%, ~60%, ~68% and ~77% of the grain boundaries in the samples annealed at 225 °C, 275 °C, 325 °C, and 350 °C for 1 h, respectively, had a high angle of misorientation (>15°). After annealing at 225 °C, the dislocations generated by the plastic deformation (DSR) were absorbed at the boundaries. At the same time, this absorption led to an increase in the misorientation. After annealing at 275 °C, however, some LAGBs are still observable

within the deformed grains, which might be attributed to the non-absorbed dislocations. In addition, the fraction of LAGBs observed in the samples after annealing at 325 °C and 350 °C led to the evolution of coarse grains surrounded by HAGBs, as shown by the arrows in Figure 6c,d.

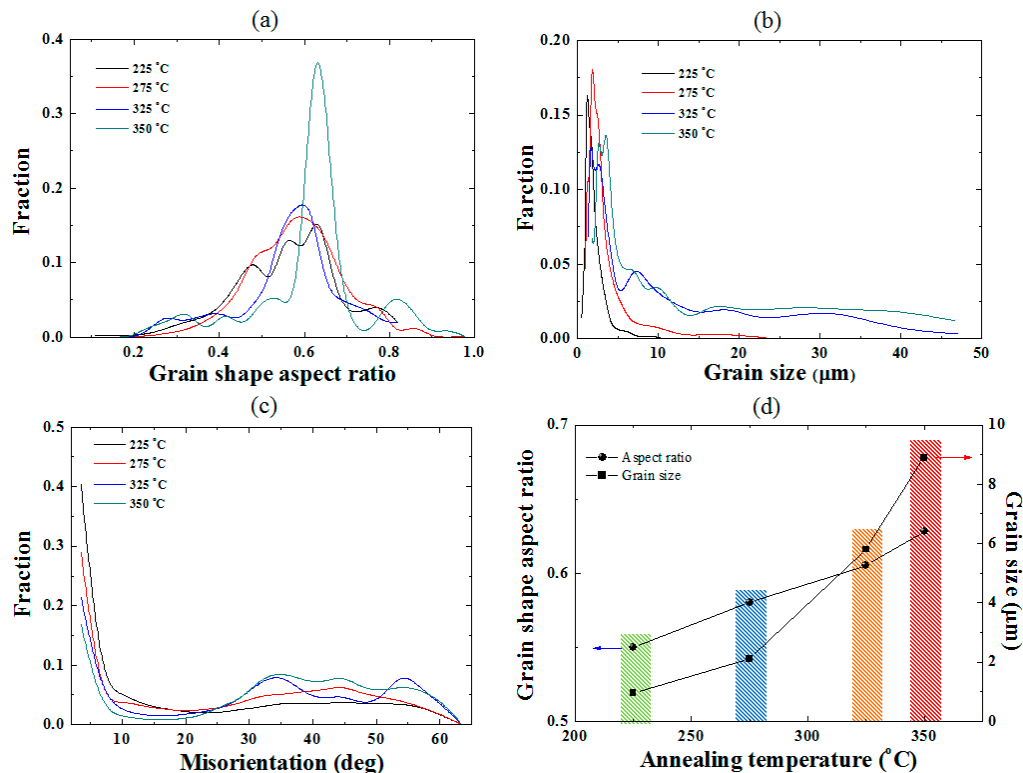


Figure 7. (a) Grain shape aspect ratio, (b) grain size, (c) grain boundaries misorientation and (d) average aspect ratio and grain size values of the DSR-deformed 6061 Al alloy annealed at different temperatures for 1 h. The columns used in Figure 7d are corresponding to the investigated samples remarked in Figure 5a.

After annealing at 225 °C, local imbalances in surface tension resulting from the transverse LAGBs can lead to pinch-off of the lamellar HAGBs formed after DSR deformation and subdivision of the elongated grains into shorter segments (Figure 8a). Examples of this behavior can be seen clearly in the high magnification TEM images presented in Figure 8b. In addition, the very fine new grains (<100 nm, indicated by the arrows in Figure 8c) observed near the grain boundaries confirmed that the recrystallization was activated after 225 °C. The recrystallized grains typically grow from nuclei formed by recovery within the rolling components [23]. Generally, the microstructure evolution during annealing of Al alloys subjected to ARB deformation is characterized by nucleation and growth [24]. However, the present results showed a different trend, in which the lamellar HAGBs pinching-off and nucleation followed by growth co-exist. This, in turn, is attributed to processing characteristics of these methods. In ARB, the sample is subjected to a high amount of strain, which enhances the recovery rate and increases the fraction of HAGBs as a result. However, in the DSR process, the quick dissipation of deformation and friction heats from a thin sheet with a high surface/volume ratio to the cold rolls lead to reduction of recovery rate. Additionally, the fraction of HAGBs achieved by the DSR is still larger than those achieved by conventional methods (symmetric cold rolling) [9]. In accordance with the previous ideas, the mechanism that is responsible for the structure evolution during annealing of the DSRed 6061 Al alloy samples is related to the medium fraction of HAGBs. At this fraction, the HAGBs pinching-off to divide the lamellar structure and nucleation at the highly-deformed areas simultaneously occur.

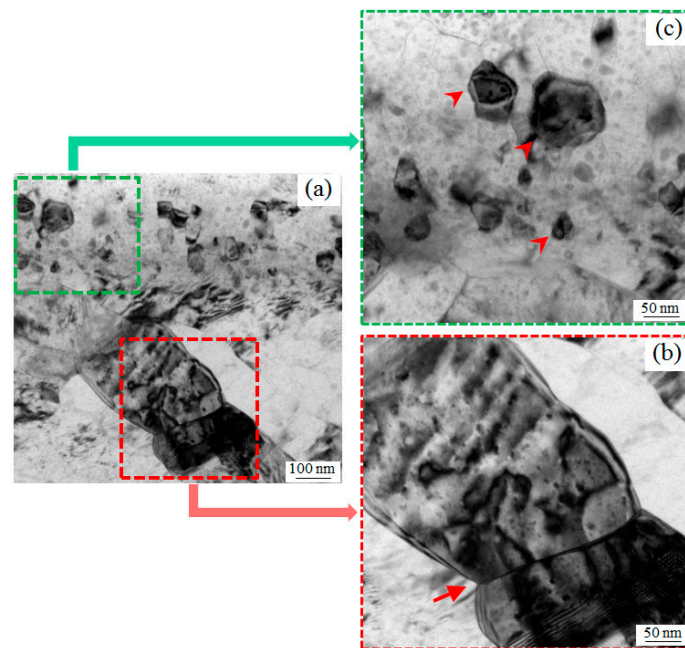


Figure 8. TEM (Transmission Electron Microscopy) images of the DSR-deformed 6061 Al alloy plates annealed at 225 °C for 1 h: (a) general microstructure; (b) pinching-off of the lamellar HAGBs (high-angle grain boundaries) formed after DSR deformation and subdivision of the elongated grains into shorter segments; (c) evolution of fine recrystallized grains.

In general, the EBSD maps and microstructural parameters of the 6061 Al alloy samples during annealing at different temperatures for 1 h showed that the microstructure evolves in a continuous manner, in that no local transformation front can be observed. This behavior was also reported by the present authors, in which the texture evolution during the annealing treatment of the DSR-deformed 6061 Al alloy samples was investigated [25]. The results showed that the manner in which the various components of rolling, shear and recrystallization textures changed, was related to the operation of continuous recrystallization.

The results presented in this work mostly involve the grain structure evolution, but the precipitation behavior upon annealing of the DSR-deformed samples, which is also one of the key aspects of the microstructure for 6xxx series Al alloys, has not been discussed. Accordingly, future experiments will be designed to address this point.

4. Conclusions

Ultrafine grained 6061 Al alloy plates (0.9 wt % Mg) manufactured by room-temperature DSR deformation were annealed isochronally at temperatures between 150 and 400 °C for 1 h. The basic results and conclusions from the present investigation are as follows:

1. The DSR-deformed 6061 Al alloy showed a lamellar boundary structure composed mostly of subgrains with high fraction of LAGBs.
2. The hardness of the DSRed plates slightly decreased with increasing temperature until 225 °C and decreased sharply after annealing at temperatures higher than 225 °C.
3. The microstructure of the DSR-fabricated plates transformed from the lamellar boundary structure into a coarse-grained structure during annealing and the extremely fine grains detected in the sample annealed at 225 °C suggested that the recrystallization became active after annealing at this temperature (225 °C).

Acknowledgments: This research was supported by National Research Foundation (NRF) of Korea (2017R1C1B5017204).

Author Contributions: Young Gun Ko conceived and designed the experiments; Kotiba Hamad performed the experiments; analyzed the data; and wrote the paper. Both authors discussed the results.

Conflicts of Interest: The authors declare no conflict of interest.

References

1. Valiev, R.Z.; Islamgaliev, R.K.; Alexandrov, I.V. Bulk nanostructured materials from severe plastic deformation. *Prog. Mater. Sci.* **2000**, *45*, 103–189. [[CrossRef](#)]
2. Ko, Y.G.; Lee, C.S.; Shin, D.H.; Semiatin, S.L. Low-temperature superplasticity of ultra-fine grained Ti-6Al-4V processed by equal-channel angular pressing. *Metall. Mater. Trans. A* **2006**, *37*, 381–391. [[CrossRef](#)]
3. Ko, Y.G.; Shin, D.H.; Park, K.T.; Lee, C.S. An analysis of the strain hardening behavior of ultra-fine grain pure titanium. *Scr. Mater.* **2006**, *54*, 1785–1789. [[CrossRef](#)]
4. Valiev, R.Z.; Langdon, T.G. Principles of equal-channel angular pressing as a processing tool for grain refinement. *Prog. Mater. Sci.* **2006**, *51*, 881–981. [[CrossRef](#)]
5. Tsuji, N.; Saito, Y.; Lee, S.H.; Minamino, Y. ARB (accumulative roll-bonding) and other new techniques to produce bulk ultrafine grained materials. *Adv. Eng. Mater.* **2003**, *5*, 338–344. [[CrossRef](#)]
6. Zhilyaev, A.P.; Langdon, T.G. Using high-pressure torsion for metal processing: Fundamentals and applications. *Prog. Mater. Sci.* **2008**, *53*, 893–979. [[CrossRef](#)]
7. Huang, X.; Suzuki, K.; Watazu, A.; Shigematsu, I.; Saito, N. Microstructure and texture of Mg-Al-Zn alloy processed by differential speed rolling. *J. Alloys Compd.* **2008**, *457*, 408–412. [[CrossRef](#)]
8. Loorentz; Ko, Y.G. Microstructure evolution and mechanical properties of severely deformed Al alloy processed by differential speed rolling. *J. Alloys Compd.* **2012**, *536*, S122–S125. [[CrossRef](#)]
9. Polkowski, W.; Jozwik, P.; Polanski, M.; Bojar, Z. Microstructure and texture evolution of copper processed by differential speed rolling with various speed asymmetry coefficient. *Mater. Sci. Eng. A* **2013**, *564*, 289–297. [[CrossRef](#)]
10. Liang, W.J.; Rometsch, P.A.; Cao, L.F.; Birbilis, N. General aspects related to the corrosion of 6xxx series aluminium alloys: Exploring the influence of Mg/Si ratio and Cu. *Corros. Sci.* **2013**, *79*, 119–128. [[CrossRef](#)]
11. Kim, W.J.; Wang, J.Y.; Choi, S.O.; Sohn, H.T. Synthesis of ultra high strength Al-Mg-Si alloy sheets by differential speed rolling. *Mater. Sci. Eng. A* **2009**, *520*, 23–28. [[CrossRef](#)]
12. Kim, J.K.; Jeong, H.G.; Hong, S.I.; Kim, Y.S.; Kim, W.J. Effect of aging treatment on heavily deformed microstructure of a 6061 aluminum alloy after equal channel angular pressing. *Scr. Mater.* **2001**, *45*, 901–907. [[CrossRef](#)]
13. Rezaei, M.; Toroghinejad, M.; Ashrafizadeh, F. Effects of ARB and ageing processes on mechanical properties and microstructure of 6061 aluminum alloy. *J. Mater. Process. Technol.* **2011**, *211*, 1184–1190. [[CrossRef](#)]
14. Hamad, K.; Chung, K.B.; Ko, Y.G. Microstructure and mechanical properties of severely deformed Mg-3%Al-1%Zn alloy via isothermal differential speed rolling at 453 K. *J. Alloys Compd.* **2014**, *615*, S590–S594. [[CrossRef](#)]
15. Hamad, K.; Ko, Y.G. A cross-shear deformation for optimizing the strength and ductility of AZ31 magnesium alloys. *Sci. Rep.* **2016**, *6*, 29954. [[CrossRef](#)] [[PubMed](#)]
16. Hamad, K.; Chung, B.K.; Ko, Y.G. Effect of deformation path on microstructure, microhardness and texture evolution of interstitial free steel fabricated by differential speed rolling. *Mater. Charact.* **2014**, *94*, 203–214. [[CrossRef](#)]
17. Hamad, K.; Megantoro, R.B.; Ko, Y.G. Microstructure and texture evolution in low carbon steel deformed by differential speed rolling (DSR) method. *J. Mater. Sci.* **2014**, *49*, 6608–6619. [[CrossRef](#)]
18. Sakai, T.; Belyakov, A.; Kaibyshev, R.; Miura, H.; Jonas, J.J. Dynamic and post-dynamic recrystallization under hot, cold and severe plastic deformation conditions. *Prog. Mater. Sci.* **2014**, *60*, 130–207. [[CrossRef](#)]
19. Hamad, K.; Ko, Y.G. Annealing characteristics of ultrafine grained low-carbon steel processed by differential speed rolling method. *Metall. Mater. Trans. A* **2016**, *47*, 2319–2334. [[CrossRef](#)]
20. Gazder, A.A.; Vu, V.Q.; Saleh, A.A.; Markovskiy, P.E.; Ivasishin, O.M.; Davies, C.H.J.; Pereloma, E.V. Recrystallisation in a cold drawn low cost beta titanium alloy during rapid resistance heating. *J. Alloys Compd.* **2014**, *585*, 245–259. [[CrossRef](#)]

21. Hazra, S.S.; Pereloma, E.V.; Gazder, A.A. Microstructure and mechanical properties after annealing of equal-channel angular pressed interstitial-free steel. *Acta Mater.* **2011**, *59*, 4015–4029. [[CrossRef](#)]
22. Hazra, S.S.; Pereloma, E.V.; Gazder, A.A. Annealing behavior and mechanical properties of severely deformed interstitial free steel. *Mater. Sci. Eng. A* **2011**, *530*, 492–503.
23. Humphreys, F.J.; Hatherly, M. *Recrystallization and Related Annealing Phenomena*, 2nd ed.; Elsevier: Amsterdam, The Netherlands, 1995.
24. Tsuji, N.; Ito, Y.; Saito, Y.; Minamino, Y. Strength and ductility of ultrafine grained aluminum and iron produced by ARB and annealing. *Scr. Mater.* **2002**, *47*, 893–899. [[CrossRef](#)]
25. Hamad, K.; Yang, H.W.; Ko, Y.G. Interpretation of annealing texture changes of severely deformed Al-Mg-Si alloy. *J. Alloys Compd.* **2016**, *687*, 300–305. [[CrossRef](#)]



© 2017 by the authors. Licensee MDPI, Basel, Switzerland. This article is an open access article distributed under the terms and conditions of the Creative Commons Attribution (CC BY) license (<http://creativecommons.org/licenses/by/4.0/>).